Electronic Supplementary Information (ESI)

Mechanistic insights into the CO₂ capture and reduction on K-promoted

Cu/Al₂O₃ by spatiotemporal *operando* methodologies

Donato Pinto,[a] Victor van der Bom Estadella [a] and Atsushi Urakawa [a]*

[1] Catalysis Engineering, Department of Chemical Engineering

Van der Maasweg 9, 2629 HZ, Delft, The Netherlands.

* Corresponding author: A.Urakawa@tudelft.nl

Catalyst characterization

X-Ray Diffraction

Ex-situ X-ray diffraction patterns were acquired to determine the crystal structure of the synthesised catalyst and to verify the outcome of the synthetic procedure.

Figure S1 reports the result obtained for the Cu-K/Al_2O_3 catalyst (Cu/K/Al_2O_3, 11/10/79 wt%). In line with previous results obtained for similar materials,[1, 2] the diffraction pattern shows reflexes typical of CuO tenorite phase (PDF 45-0937) and γ-Al_2O_3 (PDF 48-0367). The absence of strong reflexes of K_2CO_3, employed as potassium precursor in the synthesis, indicate that potassium is highly dispersed and forming an highly amorphous phase. Small broad reflexes at low angles, compatible with a $KAlCO_3(OH)_2$ phase (PDF 21-0979), indicate a strong interaction between the potassium phase and the γ-Al_2O_3 support. Such phase results from reaction of potassium carbonate with surface γ-Al_2O_3 and water absorbed on the surface during the synthesis.[3] However, this phase is crystalline at room temperature and, due to the small particle size, it is suspected to become amorphous at T = 200 °C and finally decomposing to form a K_2CO_3 phase.[4]
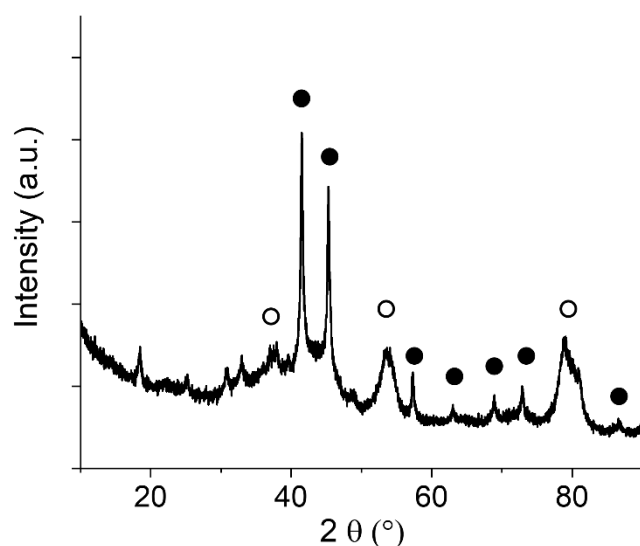

Figure S1: X-ray diffractogram of as-synthesised K-promoted Cu/Al_2O_3 (K 10 wt%, Cu 11 wt%) catalyst obtained at room temperature. Reflexes from γ-Al_2O_3 (○) and CuO tenorite (●)

BET Surface Area

The surface area of the Cu-K/Al$_2$O$_3$ was estimated by BET analysis of the fresh sample, obtaining a value of 135 m^2 g^{-1}. The surface area is considerably lower than for the unpromoted Cu/Al$_2$O$_3$ sample (Cu 12.2 wt%), for which a value of 191 m^2 g^{-1} was found. The corresponding N$_2$ adsorption-desorption isotherms obtained for the two samples are reported in Figure S2. Indeed, the impregnation of the potassium phase on highly porous material is expected to provoke pore blocking and the decrease in the catalyst surface area.[5, 6]
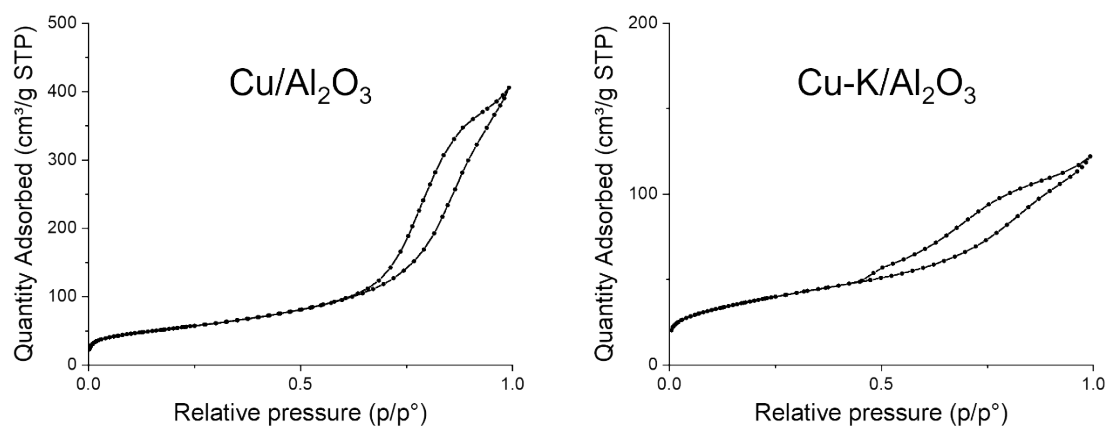

Figure S2: N$_2$ adsorption-desorption isotherms for unpromoted (left) and K-promoted (right) Cu/Al$_2$O$_3$ catalysts.

Thermogravimetric analysis

Figure S3 reports the results obtained from thermogravimetric analysis performed on the K_2CO_3 precursor, the unpromoted Cu/Al_2O_3 catalyst (Cu 12.2 wt%) and the promoted Cu-K/Al_2O_3 catalyst (11 wt% Cu, 10 wt% K). The analysis was performed by keeping the samples under H_2 flow (100 mL min^{-1} 5 vol% in Ar) in order to evaluate the weight loss induced by the reduction of the samples. After 10 minutes flushing at room temperature, the samples were heated up at at a rate of 10°C min^{-1} up to 800 °C. For the pure K_2CO_3, after a significative weight loss around 100°C related to evaporation of water adsorbed from air exposure, no weight changes are noticed until very high temperature (> 700 °C). In the Al_2O_3-supported catalysts, a weight loss from water removal from the support is associated with the contribute of CuO reduction which starts at temperatures above 250 °C. In Figure S2B, the derivative of the weight change with respect to time (dW/dT) is plotted against the sample temperature. For the unpromoted Cu/Al_2O_3 catalyst, the peak of weight loss derivative at 275 °C represents a maximum in the reduction rate ascribable to the CuO reduction process. In the Cu-K/Al_2O_3 catalyst, the presence of potassium broadens the CuO reduction peak and shifts it to higher temperatures. This phenomenon, frequently reported in literature,[7, 8] is an effect of the intimate interaction between the potassium and copper phases. After the peak referred to CuO reduction, a continuous weight loss takes place in the temperature range 350 – 800 °C, which is ascribable to the decomposition of the K_2CO_3 – derived phase on the catalyst. For the pure K_2CO_3 sample, the decomposition in H_2 starts
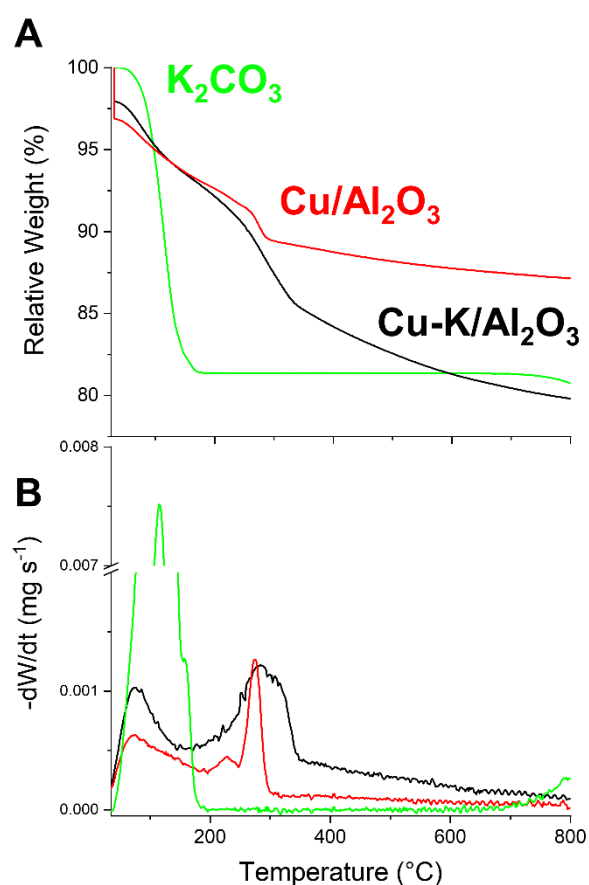

Figure S3: Thermogravimetric analysis of K_2CO_3 precursor, Cu/Al_2O_3 and Cu-K/Al_2O_3 catalysts under H_2 stream (5 vol% in Ar, 100 mL min^{-1}). Sample is kept 10 min at room temperature then heated up at 10 °C min^{-1} rate until 800°C. A) Relative weight change over temperature and B) derivative of weight loss with respect to time over temperature.

at temperature higher than 700 °C. However, in the complete catalyst, the high dispersion of potassium on γ-Al_2O_3 and the presence of metallic Cu, activating H_2, favour the decomposition of carbonates at substantially lower temperatures compared to the bulk K_2CO_3 sample.[9, 10]

Operando analysis

Spatial sampling of temperature and concentration

Figure S4 reports the complete profile of CO_2, CO and temperature measured by spatial sampling at different position in the catalytic bed. The CCR experiment was performed at 350
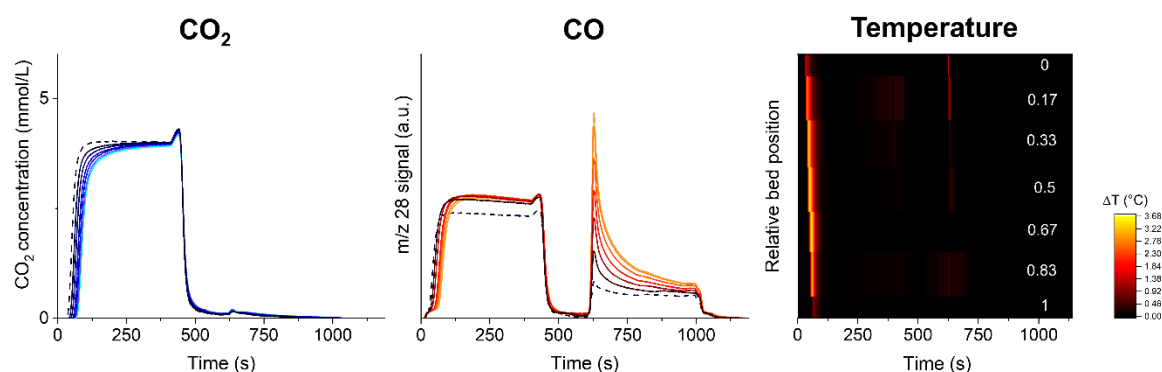

Figure S4: Spatiotemporal profile of CO_2 (left), CO (middle), and temperature (right) along the catalyst bed during CCR at 350 °C. Position 0 and 1 correspond to quartz wool at the beginning and at the end of the catalyst bed, respectively. All the positions are expressed in relative position. Profiles of different position are depicted with a colour scale from inlet of the bed (darker profile, relative position 0) towards the end of the catalytic bed (lighter profile, relative position 1).

°C, employing 0.25 g of Cu-K/Al_2O_3 catalyst.

The CO_2 concentration is evaluated by calibration of the signal at mass to charge ratio m/z = 44 of the mass spectrometer. Fragmentation of the CO_2 gives signal at m/z = 28, interfering with the detection of the CO. Due to the unsteady state nature of the pulsed experiment, it was not possible to quantify the amount of CO released in the capture phase (0 – 420 s). In contrast, the limited evolution of CO_2 in H_2 atmosphere (595 – 1015 s) permitted to use the m/z = 28 signal for quantification of the CO produced in the reduction phase, as reported in the main text.

The complete temperature profile at different position of the bed (from inlet position 0 to outlet position 1) confirms that temperature gradients are confined in the early stages of the CO_2 pulse (0 - 420 s), where the exothermic CO_2 capture takes place.

Operando DRIFTS

Figure S5 reports the result of *operando* DRIFT spectroscopy in the ν(CH) stretching region during CCR operation at 350 °C. During the CO_2 stream (0 – 420 s), the absence of bands in the ν(CH) stretching region excludes the intervention of formate species as stable intermediates derived from CO_2 capture. After switching the feed to H_2 (595 – 1015 s), bands

centered at 2670 and 2760 cm^{-1} rise with a delay compatible with the slow release of CO detected at the outlet (see main text Figure 4). Such bands are assignable to formate species on potassium,[11, 12] which would be involved in a slow hydrogenation reaction provoking the release of CO and H$_2$O observed at the outlet. Despite the low signal to noise ratio, the bands appear more intense toward the end of the bed, indicating that some gradient in the distribution of the surface species can be generated due to the packed bed configuration.

Figure S6 reports the result of *operando* DRIFT spectroscopic study in the v(CH) stretching region for the CCR experiment in which the CO$_2$ stream is substituted with a CO stream (0.5 vol% in He). The results are obtained on the same catalytic bed of Figure S4, at the same position of the results reported in Figure S4C. As can be noticed, very similar surface species dynamic is observed, with the rise of bands centered at 2670 and 2760 cm^{-1} in the H$_2$ atmosphere, associated to the tailing in the CO released by the catalyst (see main text Figure 5).
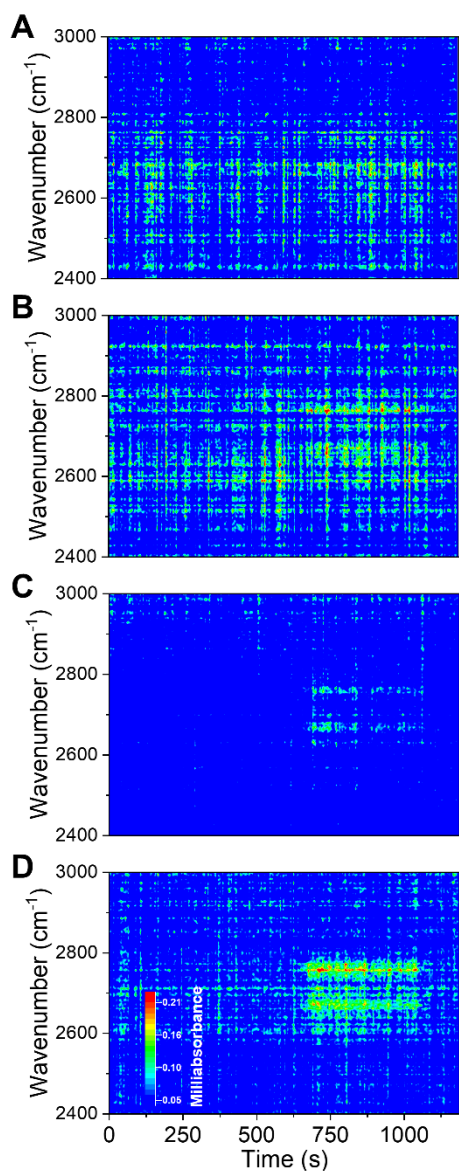
Figure S5: Dynamic evolution of surface species in the v(CH) stretching region from operando DRIFT spectroscopy during CCR at 350 °C at different position of the catalyst bed (A = 3.3 mm, B = 6.4 mm, C = 9.5 mm, D = 12.6 mm) from front (A) to back (D).
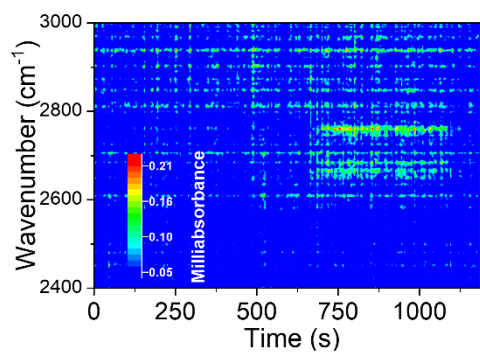

Figure S6: Dynamic evolution of surface species in the v(CH) stretching region from operando DRIFT spectroscopy during CCR at 350 °C with substitution of CO_2 with CO at the inlet.

References

1. T. Hyakutake, W. van Beek and A. Urakawa, *J. Mater. Chem. A*, 2016, **4**, 6878-6885.
2. A. Bansode, B. Tidona, P. R. von Rohr and A. Urakawa, *Catal. Sci. Technol.*, 2013, **3**, 767-778.
3. J. V. Veselovskaya, V. S. Derevschikov, T. Y. Kardash, O. A. Stonkus, T. A. Trubitsina and A. G. Okunev, *Int. J. Greenh. Gas Control.*, 2013, **17**, 332-340.
4. S. C. Lee and J. C. Kim, *Catal. Surv. Asia*, 2007, **11**, 171-185.
5. J. M. Lee, Y. J. Min, K. B. Lee, S. G. Jeon, J. G. Na and H. J. Ryu, *Langmuir*, 2010, **26**, 18788-18797.
6. X. Yang, X. Su, X. Chen, H. Duan, B. Liang, Q. Liu, X. Liu, Y. Ren, Y. Huang and T. Zhang, *Appl. Catal. B. Environ.*, 2017, **216**, 95-105.
7. G. Jacobs, T. K. Das, Y. Zhang, J. Li, G. Racoillet and B. H. Davis, *Appl. Catal. A. Gen.*, 2002, **233**, 263-281.
8. D. Courcot, C. Pruvost, E. A. Zhilinskaya and A. Aboukaïs, *Kinet. Catal.*, 2004, **45**, 580-588.
9. S. Walspurger, L. Boels, P. D. Cobden, G. D. Elzinga, W. G. Haije and R. W. van den Brink, *ChemSusChem*, 2008, **1**, 643-650.
10. M. Kantschewa, E. V. Albano, G. Etrtl and H. Kno¨zinger, *Appl. Catal.*, 1983, **8**, 71-84.
11. G. J. Millar, C. H. Rochester and K. C. Waugh, *J. Catal.*, 1995, **155**, 52-58.
12. I. L. C. Freriks, P. C. de Jong-Versloot, A. G. T. G. Kortbeek and J. P. van den Berg, *J. . Chem. Soc., Chem. Commun.*, 1986, **3**, 235-255.